



## Using Molybdenum Trioxide as a TCO Layer to Improve Performance of CdTe/CdS Thin-film Solar Cell

Bahadour Mozafari <sup>1</sup>, Ali Shahhoseini <sup>1\*</sup>

<sup>1</sup> Department of Electrical, Biomedical and Mechatronics Engineering, Qazvin Branch, Islamic Azad University, Qazvin, Iran.

Received: 28-May-2020, Accepted: 14-Jun-2020.

### Abstract

In the recent two decades, CdTe thin-film solar cells have been used due to their proper efficiency and low manufacturing cost. The transparent conducting oxide (TCO) applied in front of them has an important role in improving performance both optically and electrically. In this paper, we have used molybdenum trioxide ( $\text{MoO}_3$ ) as a TCO layer, and we also have done a comparison between this and other common TCO layers such as tin oxide ( $\text{SnO}_2$ ), zinc oxide ( $\text{ZnO}$ ) and titanium dioxide ( $\text{TiO}_2$ ) and then examined solar cell parameters in each structure. Numerical simulations of aforesaid CdTe solar cell structures have been done employing SCAPS software. Results indicate the electrical and optical parameters of CdTe/CdS solar cell with a  $\text{MoO}_3$  TCO layer which has been improved compared with other structures so that the efficiency of it reaches to 14.72%. This value is 0.64%, 0.51%, and 0.1% higher than similar cells with transparent oxide layer  $\text{SnO}_2$ ,  $\text{TiO}_2$ , and  $\text{ZnO}$ , respectively.

**Keywords:** Cadmium Telluride Thin-Film Solar Cell, Molybdenum Trioxide, TCO, SCAPS.

### 1. INTRODUCTION

The high efficiency and low manufacturing cost are two main factors in the performance evaluation of solar cells. For this purpose, various materials and techniques have been studied and investigated. CdTe thin-film

solar cell is one of the most promising photovoltaic devices in terms of efficiency and fabrication cost.

CdTe is a compound semiconductor with direct bandgap energy whose value is very close to the theoretical calculated optimum value for solar cells.

---

\*Corresponding Authors Email:  
shahhoseini@qiau.ac.ir

The direct bandgap of 1.45eV and high absorption coefficient of CdTe means that in a wide range of wavelengths from ultraviolet to CdTe bandgap (825nm), a high quantum improvement can be expected from the cell. Low wavelength photons with energy higher than bandgap energy can be absorbed by CdTe, consequently, this feature makes CdTe a suitable candidate to be employed in thin-film solar cells. Due to the high absorption coefficient of CdTe for photons with higher energy than bandgap energy, only a slight thickness (about 2 $\mu$ m to 8 $\mu$ m) of CdTe layer absorbs 99% of photons of AM1.5 solar spectrum. It is 100 times thinner than the engaged thickness in crystalline silicon solar cells for the same operation [1-3].

In a solar cell, the front layer (TCO) plays a critical role in the amount of sunlight that a cell can absorb. In this study, we have used four different TCO types in CdTe solar cells. Initially, we used 1 $\mu$ m of SnO<sub>2</sub> as a front layer and simulated the cell structure. Afterward, the same stages were repeated for simulation of cells with ZnO, TiO<sub>2</sub> and MoO<sub>3</sub> layers. Results indicates that MoO<sub>3</sub> shows better performance in CdTe solar cells compared to other TCO layers.

The SCAPS software has been used to calculate the characteristics of a CdTe solar cell. Also, the structure is composed of a layer of Cu with a work function of 5eV as a back contact, 2.5 $\mu$ m of CdTe layer as an absorber, 0.1 $\mu$ m of CdS as a window layer and finally a 1 $\mu$ m thick front contact. The main objective of this research is to investigate the effects of different kinds of TCO as a front contact on cell parameters and to introduce MoO<sub>3</sub> as the best TCO layer in

a solar cell with a view to solar cell parameters optimization [4].

## 2. NUMERICAL SOLUTION

As we know, a solar cell is basically a p-n junction whose current-voltage characteristic is located to the fourth region; meaning that the power is always delivered to the load in the aforesaid region. In a solar cell, short circuit current is equal to optical produced carriers separated and transported to external terminals. However; the amount of short circuit current decreases due to the recombination of carriers in the device.

Poisson's equations and current continuity equations for holes are considered as a main carrier transportation equation in semiconductors regardless of their junction. Poisson's equations examine distribution of filed in a device and continuity equations examine current of electrical carriers. Here, mentioned equations were simplified independent of time to:

$$\nabla(\epsilon \nabla \Psi) = -q(p - n + N_D - N_A) \quad (1)$$

$$\nabla J_n = -q(G - R) \quad (2)$$

$$\nabla J_p = +q(G - R) \quad (3)$$

where  $\epsilon$  is dielectric permittivity,  $\Psi$  is electric potential,  $q$  is electric charge,  $N_A$  is concentration of acceptor atoms,  $N_D$  is concentration of donor atoms,  $G$  is carrier generation rate,  $R$  is carrier recombination rate and  $n$ ,  $p$ ,  $J_n$  and  $J_p$  are density of electrons, density of holes, electron current density and hole current density, respectively.

In a CdTe/CdS solar cell, the CdS junction is not considered an active layer in relation to photoelectric property; in other words, it is simply a transparent window layer responsible for transporting maximum light to CdTe absorber layer [4-5]. Hence, in the study of energy band diagram for this junction, more of depletion region thickness is considered in CdTe layer.

For a cell, solving continuity equation in space charge region and neutralized region and using drift and diffusion components give the quantum efficiency of a solar cell that can be simplified as [4]:

$$\eta = 1 - \frac{\exp(-\alpha W)}{1 + \alpha L_n} \quad (4)$$

where  $\alpha$  is absorption coefficient for CdTe,  $W$  is wide of space charge region and  $L_n$  is diffusion length of electron.

### 3. STRUCTURE

Fig. 1 shows the proposed structure for simulation of a CdTe solar cell. We have adopted this structure from a literature, where SnO<sub>2</sub> has been used as a TCO with the same thickness [12]. The solar cell is affected by AM1.5 spectrum. The junction layers lie between a transparent conducting oxide as a front contact and a metal layer as a back contact.

A simulation through SCAPS software conducted to explore and compare performance of CdTe solar cells with similar parameters, but with different front layers (SnO<sub>2</sub>, TiO<sub>2</sub>, ZnO 3 MoO<sub>3</sub>). Due to the crystalline property of CdS and CdTe, their physical parameter varies depending on

growth conditions and used fabrication techniques.

In this work, parameters of absorber and window layer would not change and would be constant corresponding to Table 1 along with data in all simulation steps. For all four materials, required parameters have been given. A layer of copper with a work function of 5eV was used as a back contact. All constant parameters used in this simulation are shown in Table 1.

## 4. SIMULATION RESULTS

### 4.1. Four Parameters of The Solar Cell

Fig 2. illustrates the simulation results of four parameters of CdTe solar cells with different TCOs

As seen in Fig. 2(a) and Fig 2(b), open circuit voltage in this structure is in highest level with amount of 0.8481V. Maximum short circuit current of 22.17 mA/cm<sup>2</sup> is also achieved in a CdTe solar cell with MoO<sub>3</sub> front contact.

Moreover, CdTe solar cell with MoO<sub>3</sub> front contact has the best performance with efficiency of 14.74% compared to its counterparts as shown in Fig. 2(d).

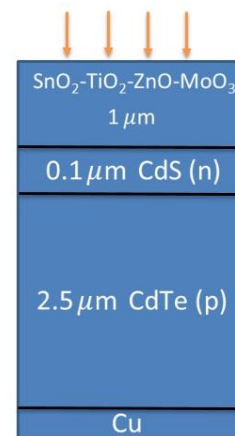
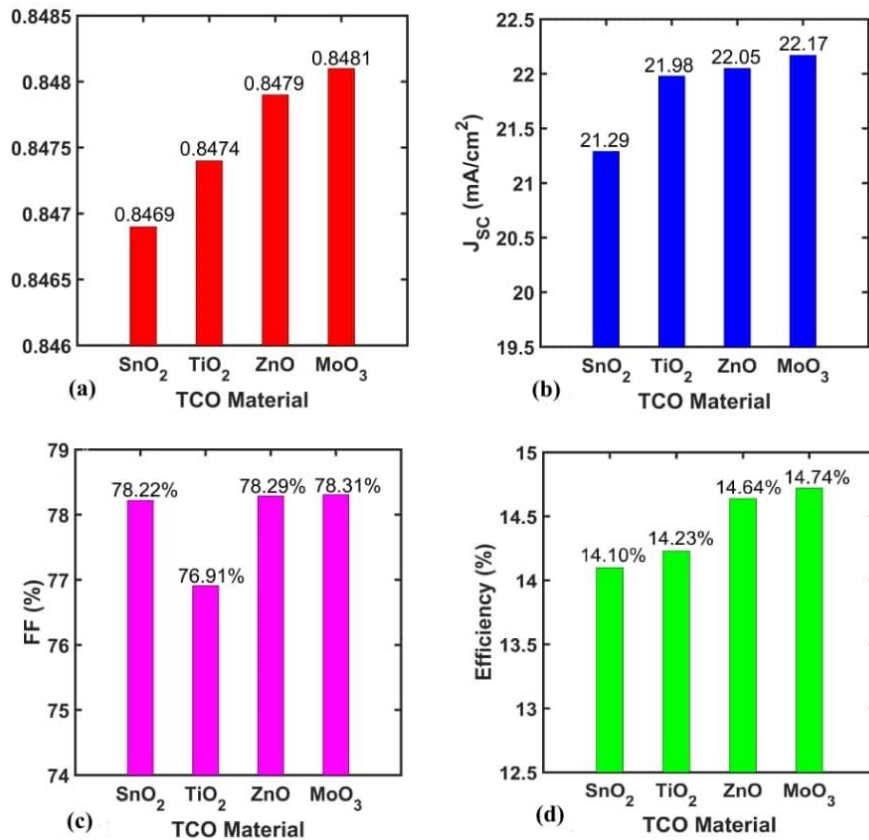
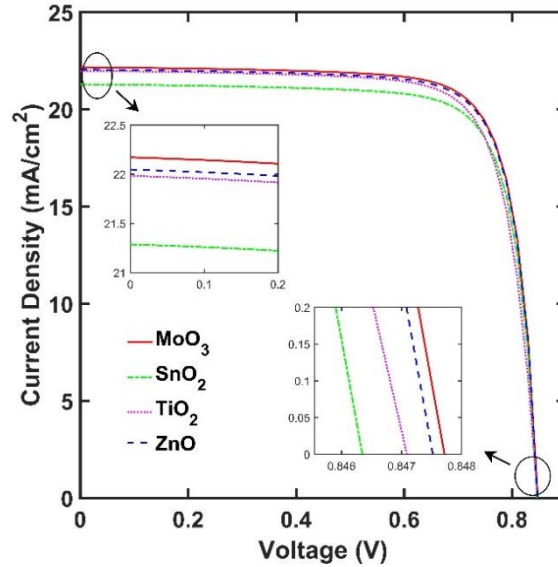


Fig. 1. Structure of a CdTe solar cell.

**Table 1. Physical parameters used in simulation.**

| Parameters                | CdS [6] | CdTe [7] | MoO <sub>3</sub> [8,13] | ZnO [9] | SnO <sub>2</sub> [10] | TiO <sub>2</sub> [11] |
|---------------------------|---------|----------|-------------------------|---------|-----------------------|-----------------------|
| $\epsilon_r$              | 4       | 9.4      | 9                       | 9       | 9                     | 9                     |
| d(nm)                     | 100     | 2500     | 1000                    | 1000    | 1000                  | 1000                  |
| $\chi_e$ (eV)             | 10      | 3.9      | 4.1                     | 4       | 4                     | 3.7                   |
| $E_g$ (eV)                | 2.4     | 1.45     | 3.8                     | 3.3     | 3.6                   | 3.26                  |
| $N_C$ (cm <sup>-3</sup> ) | 2.2E+18 | 8E+17    | 2.2E+18                 | 4E+18   | 2.2E+18               | 2E+17                 |
| $N_V$ (cm <sup>-3</sup> ) | 1.8E+19 | 1.8E+19  | 1.8E+19                 | 2E+19   | 1.8E+19               | 6E+17                 |
| $\mu_e$                   | 100     | 320      | 30                      | 100     | 100                   | 30                    |
| $\mu_p$                   | 25      | 40       | 6                       | 25      | 25                    | 6                     |
| $N_A$ (cm <sup>-3</sup> ) | 0       | 2E+14    | 0                       | 0       | 0                     | 0                     |
| $N_D$ (cm <sup>-3</sup> ) | 1.1E+18 | 0        | 1E+17                   | 1E+17   | 1E+17                 | 1E+17                 |

**Fig. 2. Solar cell parameters, (a) open circuit voltage, (b) short circuit current, (c) supply coefficient, and (d) efficiency.**



**Fig. 3. Voltage-current characteristics of a solar cell as a function of four different TCOs.**

In the following sections, we explore voltage-current characteristics and solar cell energy band to find out why molybdenum trioxide can excel compared to other types of TCO.

#### 4.2. Voltage-Current Characteristics

Fig. 3 shows voltage-current characteristics of all four structures, simultaneously. Open circuit voltage is defined on voltage axis and short circuit current is defined on current density.

#### 4.3. Energy Band Diagram of a Solar Cell

Energy band diagram of the four structures are plotted in Fig. 4. As shown, the distance from 0 to  $1\mu\text{m}$  relates to the thickness of all four types of TCO layers.

It is observed that the largest distance between the lowest of conduction band  $E_c$  and the highest of valence band  $E_v$  owns to molybdenum trioxide (red solid line), which provides the most possible entrance of light

into the cell and as a result, it will have the best optical performance in comparison with other TCOs. The thickness of 1 through  $1.1\mu\text{m}$  is associated with CdS window layer and from  $1.1\mu\text{m}$  onwards is related to CdTe absorber layer. The illuminated light on the cell generates electron-hole pair at junction region, and then the created electric-field on them separates the minority carriers and transports them to the front and back contacts. Consequently, electrons and holes move from CdTe(p) towards CdS(n) and from CdS(n) towards CdTe(p), respectively. This process creates the higher short circuit current for solar cell with MoO<sub>3</sub> TCO.

#### 4.4. Semi-Fermi Levels Energy Diagram

As illustrated in figure 5, the maximum distance between Fermi levels  $E_{Fn}$  and  $E_{Fp}$  belongs to molybdenum trioxide. The greater the distance, the higher the open circuit voltage in a solar cell, then it is concluded that one of the reasons of increasing open

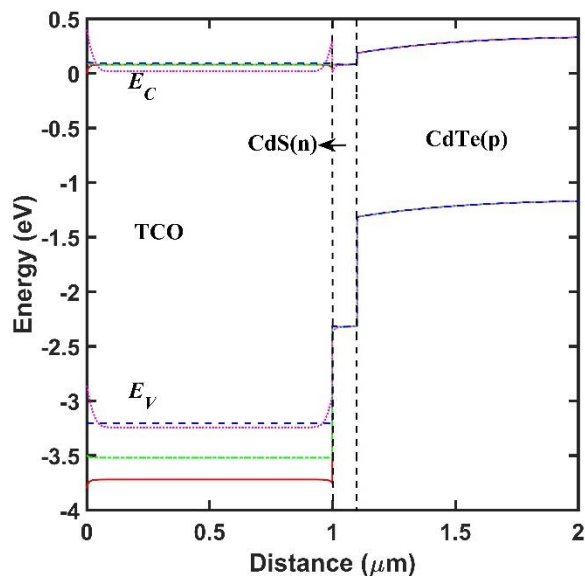


Fig. 4. Energy band diagram of a solar cell as a function of four different TCOs (The line patterns; red solid line, blue dashed line, violet dotted line and green dash-dotted line represents  $\text{MoO}_3$ ,  $\text{ZnO}$ ,  $\text{TiO}_2$  and  $\text{SnO}_2$ , respectively).

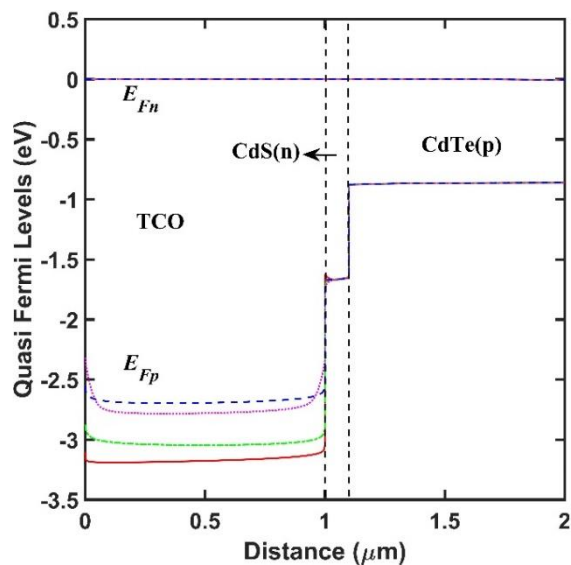


Fig. 5. Semi-Fermi levels energy diagram of a solar cell as a function of four different TCOs (The line patterns; red solid line, blue dashed line, violet dotted line and green dash-dotted line represents  $\text{MoO}_3$ ,  $\text{ZnO}$ ,  $\text{TiO}_2$  and  $\text{SnO}_2$ , respectively).

circuit voltage in CdTe solar cell is the large distance between the Fermi levels of molybdenum trioxide.

It should be noted that output parameters of a solar cell can be investigated through two

electrical and optical aspects. Electrical investigation is conducted by means of voltage-current curves, energy band diagrams and semi-Fermi levels and the optical one is done by means of quantum

efficiency diagram. By studying electrical property of a solar cell in the current section and the previous ones, it is found that a CdTe solar cell with a MoO<sub>3</sub> front contact can do better compared to other types of TCOs.

## 5. Optical Analysis of a Solar Cell

The importance of TCO in solar cell is referred more to its optical effect. As the direct light penetrates a solar cell through TCO layer, then selection of this layer is very critical.

It is evident from the energy band that ZnO falls behind its three counterparts, however, it has the greatest  $E_c$ , and thereby provides a satisfying electron velocity. According to the quantum efficiency diagram, it can be concluded that ZnO operates much better than TiO<sub>2</sub> and SnO<sub>2</sub>.

Visible spectrum illustrates that the solar cell in which MoO<sub>3</sub> is employed has the best performance among other three structures (Fig. 6). This result can be explained by high ability of MoO<sub>3</sub> than others in passing light

into the solar cell. In this case, ZnO is ranked second. This feature is noteworthy in enhancing cell parameters.

From Fig. 6, it can be seen that average quantum efficiency is calculated for the wavelength of spectrum from 300nm to 900nm. The area under curve presents average quantum efficiency of 57.67%, 55.98%, 54.59% and 54.43% for MoO<sub>3</sub>, ZnO, TiO<sub>2</sub> and SnO<sub>2</sub>, respectively which indicates an acceptable matching with cell parameters. As can be observed in Fig. 6, MoO<sub>3</sub> and ZnO operate optically much better than TiO<sub>2</sub> and SnO<sub>2</sub>.

## 6. CONCLUSION

Four different types of materials were mentioned namely MoO<sub>3</sub>, ZnO, TiO<sub>2</sub> and SnO<sub>2</sub> used as a front contact in a CdTe solar cell with similar properties. Then, for each structure, four electrical solar cell parameters e.g. open circuit voltage, short circuit current, supply coefficient, and efficiency were calculated. It was observed that the CdTe

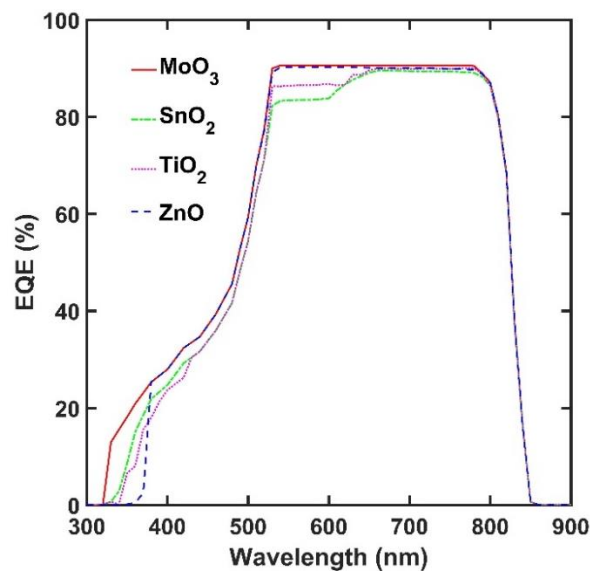


Fig. 6. Quantum efficiency diagram of a solar cell as a function of four different TCOs.

solar cell made up of MoO<sub>3</sub> has larger open circuit voltage and short circuit current compared to other mentioned materials. This results in better supply coefficient and higher efficiency for a solar cell in which MoO<sub>3</sub> is used.

The results obtained from quantum efficiency diagram indicate that a solar cell can absorb the highest amount of light spectrum by using MoO<sub>3</sub> as a front contact material. This phenomenon leads to more electron-hole production, and increases the short circuit current, accordingly.

## REFERENCES

- [1] S. M. Sze, Kwok K.ng, "Physics of Semiconductor Devices", 3rd edition. Wiley, New York, 2007.
- [2] I. Fauzi, M. Mohamad Shahimin and M. Mazalan, "Simulation of cadmium telluride solar cells structure", *2010 IEEE Student Conference on Research and Development (SCoReD)*, 2010.
- [3] M. Mannan, M. Anjan and M. Kabir, "Modeling of current–voltage characteristics of thin film solar cells", *Solid-State Electronics*, vol. 63, no. 1, pp. 49-54, 2011.
- [4] L. Kosyachenko, A. Savchuk and E. Grushko, "Dependence of the efficiency of a CdS/CdTe solar cell on the absorbing layer's thickness", *Semiconductors*, vol. 43, no. 8, pp. 1023-1027, 2009.
- [5] V. Shukla and G. Panda, "The performance study of CdTe/CdS/SnO<sub>2</sub> solar cell", *Materials Today: Proceedings*, 2020.
- [6] R. Safa Sultana, A. Bahar, M. Asaduzzaman and K. Ahmed, "Numerical modeling of a CdS/CdTe photovoltaic cell based on ZnTe BSF layer with optimum thickness of absorber layer", *Cogent Engineering*, vol. 4, no. 1, 2017.
- [7] F. Anwar, S. Afrin, S. Sarwar-Satter, R. Mahbub and S. Mahmud-Ullah, "Simulation and Performance Study of Nanowire CdS/CdTe Solar Cell", *International Journal of Renewable Energy Research-IJREER*, vol. 7, no. 2, pp. 885-893, 2017.
- [8] I. Samatov, B. Jeppesen, A. Larsen and S. Ram, "Room-temperature rf-magnetron sputter-deposited W-doped indium oxide: decoupling the influence of W dopant and O vacancies on the film properties", *Applied Physics A*, vol. 122, no. 4, 2016.
- [9] M. Rahman, S. Rahman, S. Ahmed and M. Hoque, "Numerical analysis of CdS:O/CdTe thin film solar cell using Cu<sub>2</sub>Te BSF layer", *2016 9th International Conference on Electrical and Computer Engineering (ICECE)*, 2016.
- [10] A. Belfar, "The role of p+-layer dopant concentration, p+-layer band gap and p+-layer thickness in the performances of a-Si:H n – i – p – p+ solar cells with double layer window nanocrystalline silicon", *Optik*, vol. 126, no. 24, pp. 5688-5693, 2015.
- [11] S. Khosroabadi, S. Keshmiri and S. Marjani, "Design of a high efficiency CdS/CdTe solar cell with optimized step doping, film thickness, and carrier lifetime of the absorption layer",



*Journal of the European Optical Society: Rapid Publications*, vol. 9, 2014.

- [12] L. Cruz, L. Kazmerski, H. Moutinho, F. Hasoon, R. Dhere and R. de Avillez, "The influence of post-deposition treatment on the physical properties of CdTe films deposited by stacked elemental layer processing", *Thin Solid Films*, vol. 350, no. 1-2, pp. 44-48, 1999.
- [13] F. Wang, Z. Tan and Y. Li, "Solution-processable metal oxides/chelates as electrode buffer layers for efficient and stable polymer solar cells", *Energy & Environmental Science*, vol. 8, no. 4, pp. 1059-1091, 2015.